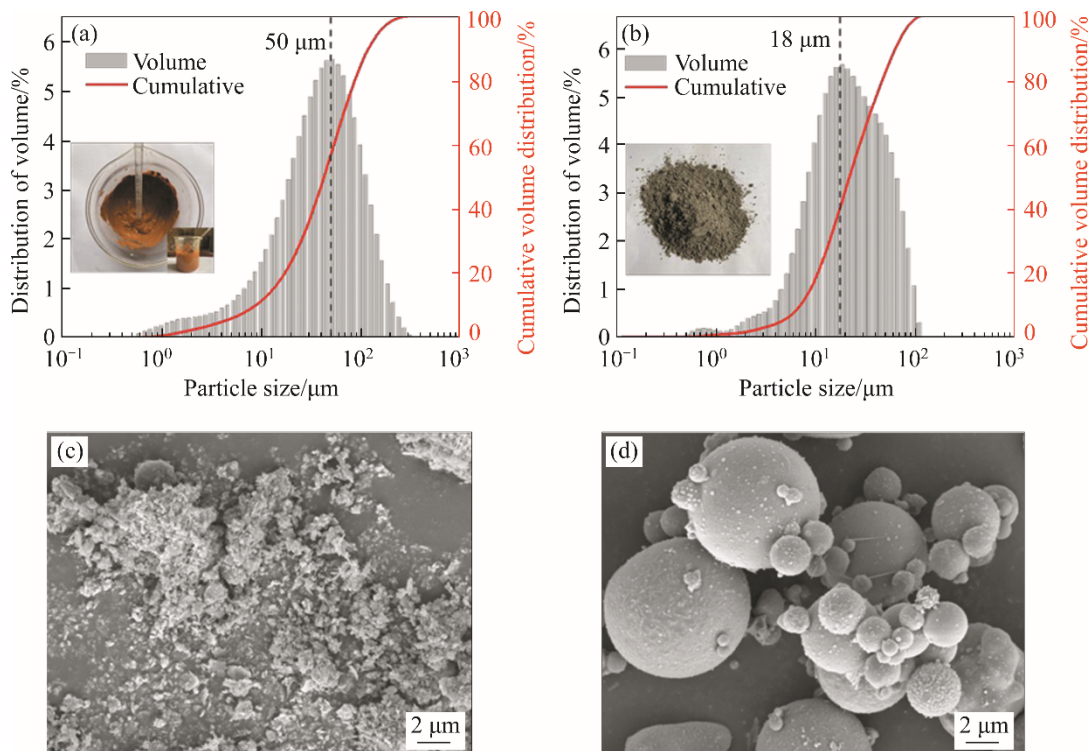


## Supplementary information

**Table S1** Source and density of raw materials

Raw materials	Source	Density/(g·cm <sup>-3</sup> )
BT slurry	Bauxite discharge of CHALCO Guangxi	1.83
FA	Guixi Power Plant in Guangxi Zhuang Autonomous Region	2.61



**Figure S1** Particle size distribution and microstructure of (a, c) BTs and (b, d) FA

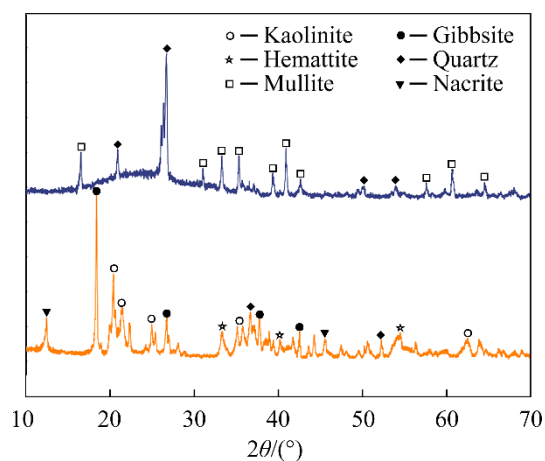


**Figure S2** The XRD patterns of BTs and FA

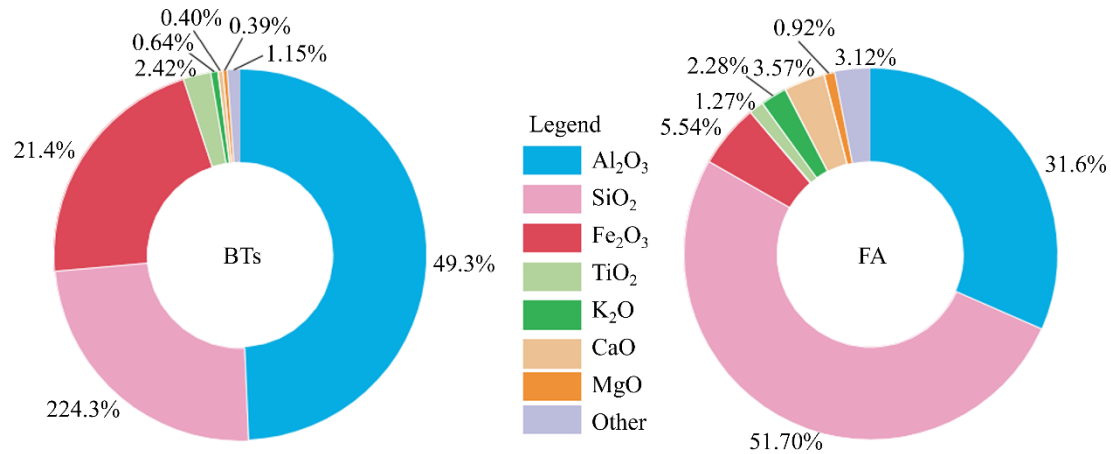


**Figure S3** Chemical compositions of BTs and FA

**Table S2** Test design

Sample	w/o				L/S ratio
	BTs	FA	H <sub>2</sub> O <sub>2</sub> admixture	NaOA admixture	
B4F0	100	0	8	0.5	0.5
B3F1	75	25	8	0.5	0.5
B2F2	50	50	8	0.5	0.5
B1F3	25	75	8	0.5	0.5
L/S-0.45	50	50	8	0.5	0.45
L/S-0.55	50	50	8	0.5	0.55
L/S-0.6	50	50	8	0.5	0.6
H <sub>2</sub> O <sub>2</sub> -0	50	50	0	0.5	0.5
H <sub>2</sub> O <sub>2</sub> -4	50	50	4	0.5	0.5
H <sub>2</sub> O <sub>2</sub> -6	50	50	6	0.5	0.5
H <sub>2</sub> O <sub>2</sub> -10	50	50	10	0.5	0.5
NaOA-0	50	50	8	0	0.5
NaOA-0.3	50	50	8	0.3	0.5
NaOA-0.8	50	50	8	0.8	0.5
NaOA-1	50	50	8	1	0.5

**Specific synthesis details:** TPGs with different characteristics were synthesized by adjusting BT content, H<sub>2</sub>O<sub>2</sub> admixture, L/S ratio, and foam stabilizer admixture. Sodium silicate (Na<sub>2</sub>SiO<sub>4</sub>) anhydrous powder (SiO<sub>2</sub>/Na<sub>2</sub>O molar ratio of 2, 99% purity, Usolf Technology) was dissolved in water at room temperature ((20±2) °C), the molar ratio was adjusted to 1 by adding sodium hydroxide (NaOH, AR), and Na<sub>2</sub>SiO<sub>4</sub> solid content was adjusted to 30% with water. As the BT slurry contains water, the actual water addition was calculated by subtracting the water content in the BT slurry from the total required water. The mixtures were sealed and then allowed to stand for 24 h. Then, the Na<sub>2</sub>SiO<sub>4</sub> solution was introduced into the BT slurry, FA, and foam stabilizer (C<sub>18</sub>H<sub>33</sub>NaO<sub>2</sub>, NaOA, 98% purity) mixture, followed by stirring the resultant mixture at a speed of 300 r/min for 10 min to form a slurry. Then, the diluted solution of 10 wt.% H<sub>2</sub>O<sub>2</sub> was added to the mixture and stirred in a stirrer at 200–300 r/min for 1 min to form a paste. Finally, the paste was poured into a 70.7 mm×70.7 mm×70.7 mm mold to make a specimen.

**Table S3** Source and density of raw materials

	Model	Formulas	Description
Isothermal model [1]	Langmuir	$q_e = \frac{q_m b C_e}{1 + b C_e}$	Considering the finite adsorption and solute mass on the solid surface.
	Freundlich	$q_e = K_F C_e^{1/n}$	Adsorption processes occurring on non-homogeneous surfaces.
Kinetic model [2]	Pseudo-first-order model	$q_t = q_e (1 - e^{-k_1 t})$	The rate of adsorption is directly proportional to the concentration of unadsorbed material.
	Pseudo-second-order model	$q_t = \frac{k_2 q_e^2 t}{1 + k_2 q_e t}$	The rate of adsorption is proportional to the square of the unadsorbed material.

Note: where  $q_m$  is the maximum adsorption capacity (mg/g);  $b$  is the adsorption constant;  $K_F$  is the Freundlich constant;  $n$  is the adsorption constant related to the binding energy;  $t$  is the contact time;  $q_t$  and  $q_e$  are the amounts of  $Pb^{2+}$  and  $Cu^{2+}$  on TPG at moment  $t$  and equilibrium (mg/g), respectively; and  $k_1$  and  $k_2$  are the adsorption rate constants for the two models.

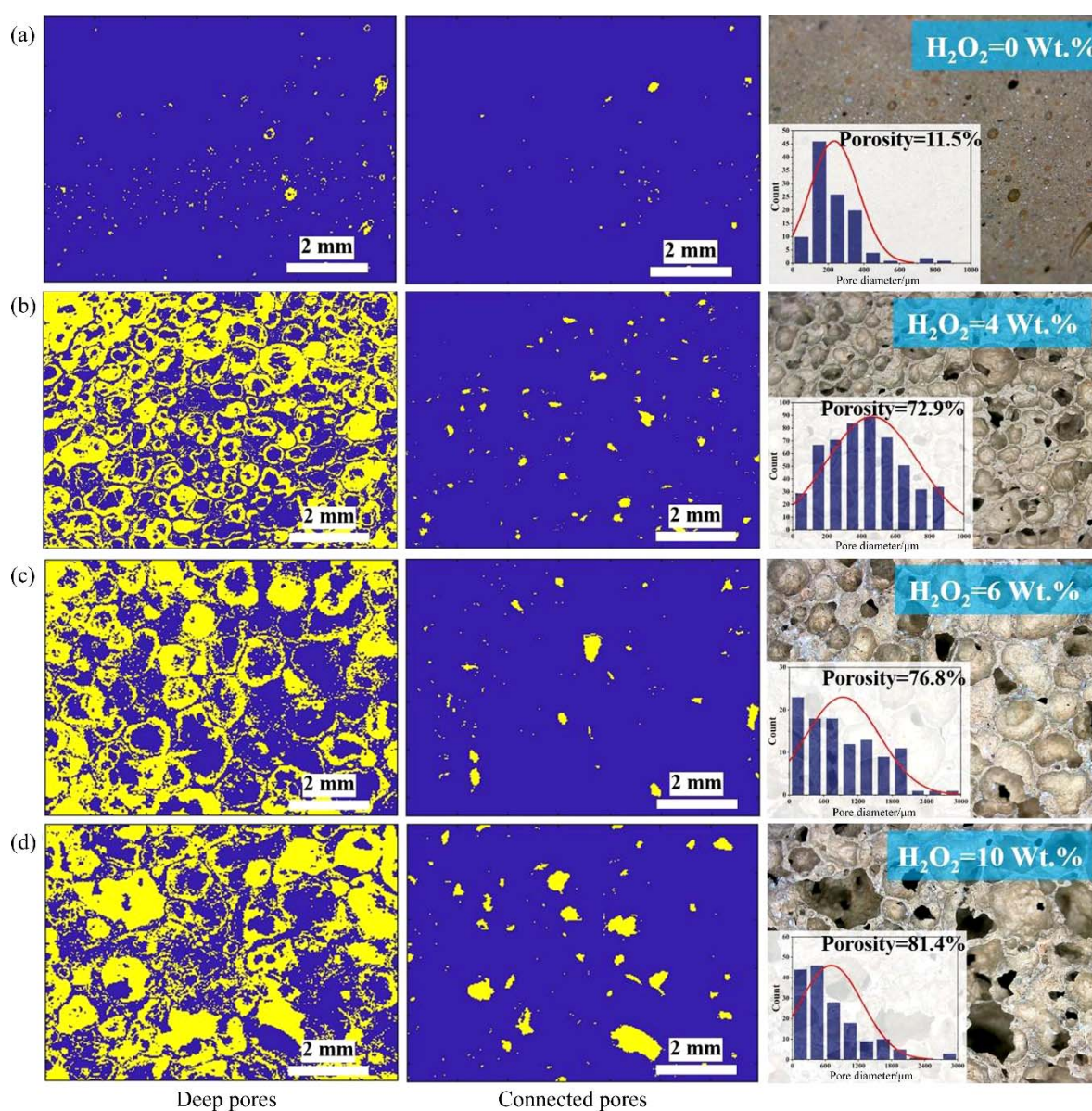
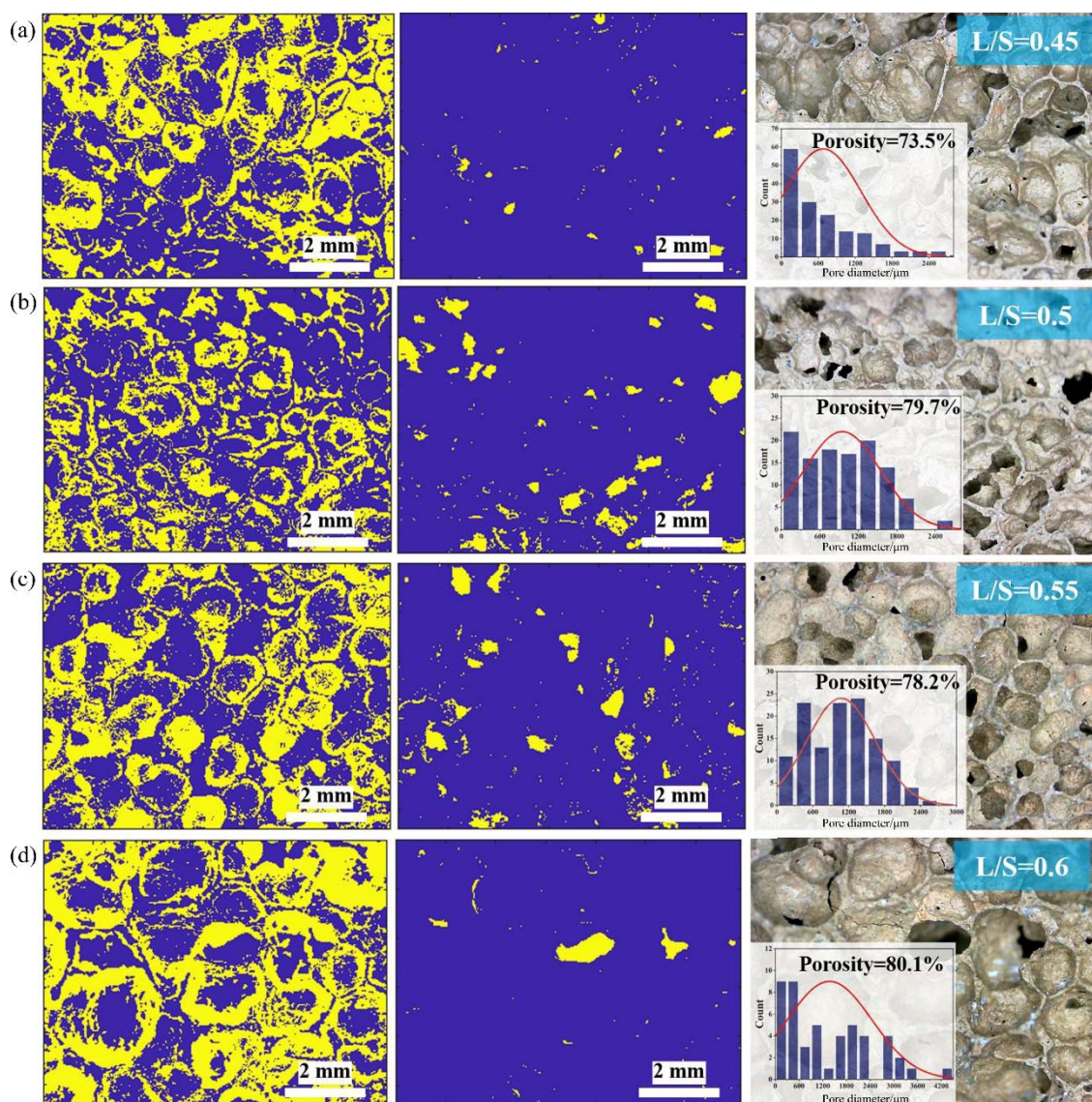


**Figure S4** Typical segmentation of pore structure images and statistical pore size distribution of TPG with different  $H_2O_2$  admixture: (a) 0 wt.%; (b) 4 wt.%; (c) 6 wt.%; (d) 10 wt.%



Deep pores

Connected pores

**Figure S5** Typical segmentation of pore structure images and statistical pore size distribution of TPG with different L/S ratios: (a) 0.45; (b) 0.5; (c) 0.55; (d) 0.6

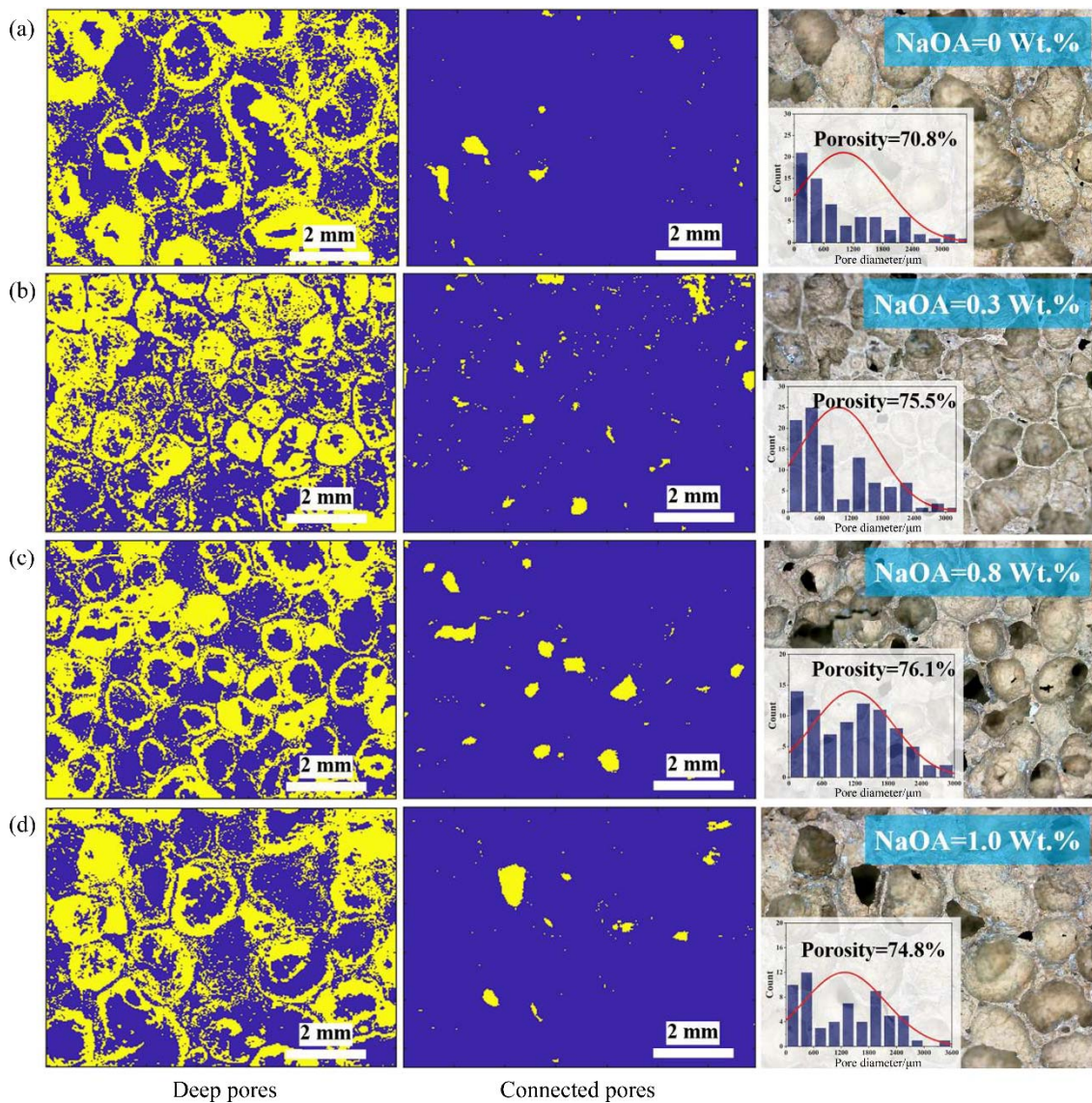


**Figure S6** Typical segmentation of pore structure images and statistical pore size distribution of TPG with different NaOA admixture: (a) 0 wt.%; (b) 0.3 wt.%; (c) 0.8 wt.%;(d) 1 wt.%

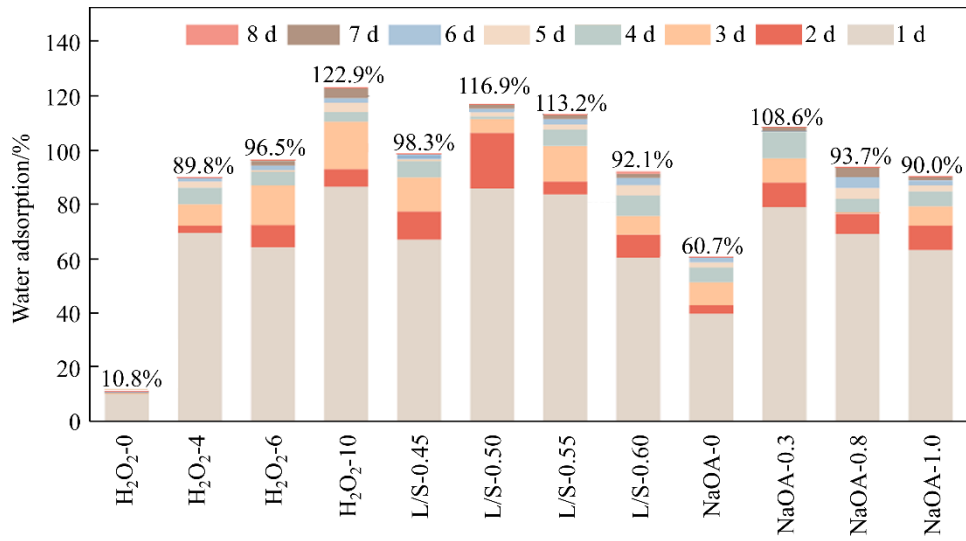


**Figure S7** The variation of water absorption rate over time for different TPG samples

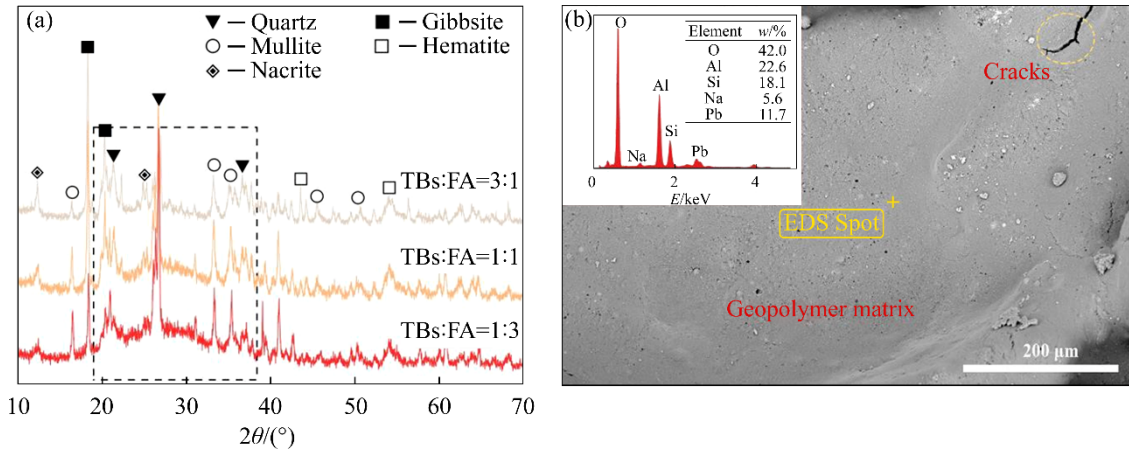


**Figure S8** (a) XRD patterns of TPG samples with different BT contents and (b) SEM images of H<sub>2</sub>O<sub>2</sub>-0 after Pb<sup>2+</sup> adsorption

**Table S4** Fitting parameters for adsorption isotherm models

Element	Langmuir			Freundlich		
	$q_m/(\text{mg}\cdot\text{g}^{-1})$	$b$	$R^2$	$K_F/(\text{mg}\cdot\text{g}^{-1})$	$1/n$	$R^2$
Pb	46.33	0.16	0.943	13.29	0.27	0.926
Cu	48.68	0.09	0.990	11.47	0.30	0.928

**Table S5** Adsorption capacity of different types of geopolymers for the removal of Pb<sup>2+</sup> or Cu<sup>2+</sup> reported in the literature

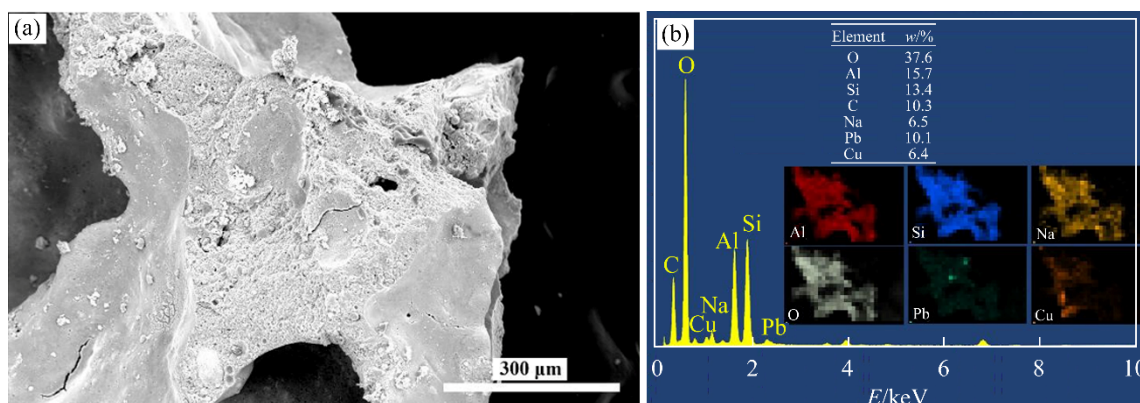
Adsorbent	Type	Heavy metal	Maximum adsorption capacity/(mg·g <sup>-1</sup> )	Reference
Zeolite-based geopolymer	Powder	Cu	52.6	[3]
Gold mine tailings based geopolymer	Powder	Cu	46.3	[4]
FA-based geopolymer	Powder	Cu	40.0	[5]
Metakaolin-based inorganic polymer spheres	Bulk	Cu	34.5	[6]
Slag-based geopolymer	Powder	Pb	629.21	[7]
Metakaolin-based geopolymers	Bulk	Pb	35.0	[8]
Metakaolin/red mud-derived geopolymer	Bulk	Pb	30.7	[9]
FA-based geopolymer	Bulk	Pb	6.3	[10]

**Table S6** Fitting parameters for kinetics model

Element	PF-order			PS-order		
	q <sub>e</sub> /(mg·g <sup>-1</sup> )	k <sub>1</sub>	R <sup>2</sup>	q <sub>e</sub> /(mg·g <sup>-1</sup> )	k <sub>2</sub>	R <sup>2</sup>
Pb	23.16	1.12	0.954	24.42	0.07	0.956
Cu	21.99	0.78	0.947	23.48	0.05	0.992

**Table S7** The removal efficiency and desorption efficiency of Pb<sup>2+</sup> and Cu<sup>2+</sup> by geopolymers

Element	Removal efficiency/%					Desorption efficiency/%				
	1	2	3	4	5	1	2	3	4	5
Pb	94.82	62.13	50.94	29.65	32.39	8.35	10.29	16.73	21.64	20.35
Cu	91.41	57.69	43.24	35.31	34.77	17.69	15.33	19.24	24.72	24.41

**Figure S9** SEM image, EDS spectrum and elemental distribution after adsorption of Pb<sup>2+</sup> and Cu<sup>2+</sup>

## References

- [1] GRAIMED B H, ABD ALI Z T. Batch and continuous study of one-step sustainable green graphene sand hybrid synthesized from Date-syrup for remediation of contaminated groundwater [J]. Alexandria Engineering Journal, 2022, 61(11): 8777–8796. DOI: 10.1016/j.aej.2022.02.018.
- [2] KYZAS G Z, BIKIARIS D N, MITROPOULOS A C. Chitosan adsorbents for dye removal: A review [J]. Polymer International, 2017, 66(12): 1800–1811. DOI: 10.1002/pi.5467.
- [3] BAYKARA H, DE LOURDES MENDOZA SOLORZANO M, DELGADO ECHEVERRIA J J, et al. The use of zeolite-based geopolymers as adsorbent for copper removal from aqueous media [J]. Royal Society Open Science, 2022, 9(3): 211644. DOI: 10.1098/rsos.211644.
- [4] DEMIR F, MOROYDOR DERUN E. Usage of gold mine tailings based geopolymer on Cu<sup>2+</sup> adsorption from water [J]. Main Group Chemistry, 2019, 18(4): 467–476. DOI: 10.3233/mgc-190801.
- [5] DARMAYANTI L, KADJA G T M, NOTODARMOJO S, et al. Structural alteration within fly ash-based geopolymers governing the adsorption of Cu<sup>2+</sup> from aqueous environment: Effect of alkali activation [J]. Journal of Hazardous Materials, 2019, 377: 305–314. DOI: 10.1016/j.jhazmat.2019.05.086.

- [6] TANG Qing, GE Yuan-yuan, WANG Kai-tuo, et al. Preparation and characterization of porous metakaolin-based inorganic polymer spheres as an adsorbent [J]. *Materials & Design*, 2015, 88: 1244–1249. DOI: 10.1016/j.matdes.2015.09.126.
- [7] TANG Qing, WANG Kai-tuo, YASEEN M, et al. Synthesis of highly efficient porous inorganic polymer microspheres for the adsorptive removal of Pb<sup>2+</sup> from wastewater [J]. *Journal of Cleaner Production*, 2018, 193: 351–362. DOI: 10.1016/j.jclepro.2018.05.094.
- [8] LÓPEZ F J, SUGITA S, TAGAYA M, et al. Metakaolin-based geopolymers for targeted adsorbents to heavy metal ion separation [J]. *Journal of Materials Science and Chemical Engineering*, 2014, 2(7): 16–27. DOI: 10.4236/msce.2014.27002.
- [9] CARVALHEIRAS J A, NOVAIS R M, LABRINCHA J A A. Metakaolin/red mud-derived geopolymer monoliths: Novel bulk-type sorbents for lead removal from wastewaters [J]. *Applied Clay Science*, 2023, 232: 106770. DOI: 10.1016/j.clay.2022.106770.
- [10] NOVAIS R M, BURUBERRI L H, SEABRA M P, et al. Novel porous fly-ash containing geopolymer monoliths for lead adsorption from wastewaters [J]. *Journal of Hazardous Materials*, 2016, 318: 631–640. DOI: 10.1016/j.jhazmat.2016.07.059.